J. Plasma Fusion Res. SERIES, Vol.6 (2004) 618–621

Computer Simulation of Fishbone Oscillation

SHIOZAKI Yutaka and TODO Yasushi[1]
Graduate University for Advanced Studies, Toki, 509-5292, Japan
[1]National Institute for Fusion Science, Toki, 509-5292, Japan
(Received: 9 December 2003 / Accepted: 9 August 2004)

Abstract

Particle-magnetohydrodynamic (MHD) hybrid simulations were carried out to investigate nonlinear evolution of precessional fishbone instability using parameters similar to the PDX experiment. Spatial profile of the fishbone mode is different from that of the kink mode. The fishbone mode frequency shifts downward at saturation of the instability, while it is close to the experimental value in the linear growth phase. The saturation level of the plasma displacement is comparable to the radius of the $q = 1$ surface.

Keywords:
precessional fishbone instability, computer simulation, frequency chirping

1. Introduction

Fishbone instability was first observed during near-perpendicular neutral beam injection in the PDX tokamak [1]. The instability takes place in recurrent bursts, accompanied by frequency decrease during each burst. Two types of fishbone modes, precessional fishbones [2] and thermal ion diamagnetic drift fishbones [3], were theoretically predicted. Nonlinear simulations of the thermal ion diamagnetic drift fishbones were carried out in Ref. [4] where a perturbative description was applied. On the other hand, little is known about self-consistent nonlinear evolution of the precessional fishbones. Perturbative approach is not valid for the precessional fishbones, since the mode frequency emerges from the shear Alfvén continuous spectrum and depends intrinsically on the energetic ion distribution. This makes the problem more difficult and interesting than the thermal ion diamagnetic drift fishbones. We carried out particle-MHD hybrid simulations with parameters similar to the PDX experiments. This is the first simulation of the precessional fishbone that demonstrates the saturation of the instability and decrease in the mode frequency.

In Sec. **2**, simulation model and method are described. Simulation results are reported in Sec. **3**. Section **4** is devoted to disccussion and summary.

2. Simulation model

In the particle-MHD hybrid simulation model [5] plasma is divided into two parts, bulk plasma and energetic ions. The bulk plasma is described by the ideal MHD equations. Two fluid effects which might be important to the kink and fishbone instabilities are not taken into account in the present study. Electromagnetic field is given by the MHD description. This approximation is reasonable under the condition that the energetic ion density is much less than the bulk plasma density. The ideal MHD equations are,

$$\frac{\partial \rho}{\partial t} = -\nabla\cdot\left(\rho \boldsymbol{v}\right), \tag{1}$$

$$\rho\frac{\partial}{\partial t}\boldsymbol{v} + \rho\boldsymbol{v}\cdot\nabla\boldsymbol{v} = -\nabla p + \frac{1}{\mu_0}(\nabla\times\boldsymbol{B})\times\boldsymbol{B}, \tag{2}$$

$$\frac{\partial \boldsymbol{B}}{\partial t} = -\nabla\times\boldsymbol{E}, \tag{3}$$

$$\frac{\partial p}{\partial t} = -\nabla\cdot\left(p\,\boldsymbol{v}\right) - \left(\gamma - 1\right)p\,\nabla\cdot\boldsymbol{v}, \tag{4}$$

$$\boldsymbol{E} = -\boldsymbol{v}\times\boldsymbol{B} \tag{5}$$

where μ_0 is the vacuum magnetic permeability, γ is the adiabatic constant, ρ is the mass density, $\boldsymbol{v}$ is the velocity, and p is the pressure. The MHD equations are solved using a finite difference scheme of 4th order accuracy in space and time.

The drift-kinetic description is employed for the energetic ions which are generated by the neutral beam injection. The guiding-center velocity $\boldsymbol{u}$ is given by

$$\boldsymbol{u} = \boldsymbol{v}_{\parallel}^{*} + \boldsymbol{v}_{E} + \boldsymbol{v}_{B}, \tag{6}$$

$$\boldsymbol{v}_{\parallel}^{*} = \frac{v_{\parallel}}{B}\left[\boldsymbol{B} + \rho_{\parallel}B\nabla\times\mathbf{b}\right], \tag{7}$$

$$\boldsymbol{v}_{E} = \frac{1}{B}\left[\boldsymbol{E}\times\mathbf{b}\right], \tag{8}$$

$$\boldsymbol{v}_{B} = \frac{1}{q_h B}\left[-\mu\nabla B\times\mathbf{b}\right], \tag{9}$$

$$\rho_{\parallel} = \frac{m_h v_{\parallel}}{q_h B}, \tag{10}$$

$$m_h v_{\parallel}\frac{\mathrm{d}v_{\parallel}}{\mathrm{d}t} = \boldsymbol{v}_{\parallel}^{*}\cdot\left[q_h\boldsymbol{E} - \mu\nabla B\right], \tag{11}$$

Corresponding author's e-mail: shiozaki@toki.theory.nifs.ac.jp

where $v_\parallel$ is the velocity parallel to the magnetic field, μ is the magnetic moment, m_h and q_h are mass and charge of an energetic ion, and $\mathbf{b}$ is a unit vector paralell to $\boldsymbol{B}$. The effects of the energetic ions on the bulk plasma are taken into account in the MHD momentum equation:

$$\rho \frac{\partial}{\partial t}\boldsymbol{v} + \rho \boldsymbol{v}\cdot\nabla\boldsymbol{v} = \left(Q - Q_h\right)\boldsymbol{E} + \left(\frac{1}{\mu_0}\nabla\times\boldsymbol{B} - \boldsymbol{j}_h\right)\times\boldsymbol{B} - \nabla p, \quad (12)$$

where Q and Q_h are the total charge density and energetic-ion charge density, and $\boldsymbol{j}_h$ is the energetic-ion current density. The total charge density Q is negligible in the MHD approximation where the quasineutrality is satisfied. Paying attention to the fact that $-Q_h\boldsymbol{E}$ cancel out with the Lorentz force due to $\boldsymbol{E}\times\boldsymbol{B}$ current of the energetic ions, Eq. (12) is rewritten to

$$\rho \frac{\partial}{\partial t}\boldsymbol{v} + \rho \boldsymbol{v}\cdot\nabla\boldsymbol{v} = \left(\frac{1}{\mu_0}\nabla\times\boldsymbol{B} - \boldsymbol{j}_h'\right)\times\boldsymbol{B} - \nabla p, \quad (13)$$

$$\begin{aligned}\boldsymbol{j}_h' &\equiv \int\left(\boldsymbol{v}_\parallel^* + \boldsymbol{v}_B\right) f \mathrm{d}^3 v + \nabla\times\boldsymbol{M} \\ &= \boldsymbol{j}_{h\parallel} + \frac{1}{B}\left(P_{h\parallel}\nabla\times\mathbf{b} - P_{h\perp}\nabla\ln B\times\mathbf{b}\right) - \nabla\times\left(\frac{P_{h\perp}}{B}\mathbf{b}\right),\end{aligned} \quad (14)$$

$$\boldsymbol{M} = -\int \mu\mathbf{b} f \mathrm{d}^3 v, \quad (15)$$

where $\nabla\times\boldsymbol{M}$ is the energetic ion magnetized current, $P_{h\parallel}$ and $P_{h\perp}$ are the energetic ion parallel pressure and perpendicular pressure, respectively. For the initial distribution, the energetic ions are assumed to be isotropic in the velocity space. Equation (13) has an exact simple form for isotropic energetic ion distributions,

$$\rho \frac{\partial}{\partial t}\boldsymbol{v} + \rho \boldsymbol{v}\cdot\nabla\boldsymbol{v} = \frac{1}{\mu_0}(\nabla\times\boldsymbol{B})\times\boldsymbol{B} - \nabla P_h - \nabla p. \quad (16)$$

The δf particle simulation method [6] is applied to the energetic ions. Time evolution of the j-th particle's weight, w_j, is described by

$$\frac{\mathrm{d}}{\mathrm{d}t}\omega_j = -(1-\omega_j)\left[\left(\boldsymbol{v}_E + v_\parallel\ \delta\mathbf{b}\right)\cdot\nabla + \left(\frac{\mathrm{d}v_\parallel}{\mathrm{d}t}\right)_1\frac{\partial}{\partial v_\parallel}\right]\ln f_0, \quad (17)$$

$$\left(\frac{\mathrm{d}v_\parallel}{\mathrm{d}t}\right)_1 = \left[\mathbf{b} + \rho_\parallel\nabla\times\mathbf{b}\right]\cdot\left[\frac{q_h}{m_h}\boldsymbol{E}\right] + \delta\mathbf{b}\cdot\left[-\frac{\mu}{m_h}\nabla B\right], \quad (18)$$

$$\delta\mathbf{b} = \mathbf{b} - \mathbf{b}_0, \quad (19)$$

where f_0 is the initial distribution which is a function of the magnetic surface and energy. Using this weight, the energetic ion current $\boldsymbol{j}_h'$ in Eq. (14) is evaluated through

$$P_{h\parallel} = P_{h\parallel 0} + \sum_j \omega_j m_h v_{\parallel j}^2 S\left(\boldsymbol{x} - \boldsymbol{X}_j\right), \quad (20)$$

$$P_{h\perp} = P_{h\perp 0} + B\sum_j \omega_j \mu_j S\left(\boldsymbol{x} - \boldsymbol{X}_j\right), \quad (21)$$

where $S(\boldsymbol{x} - \boldsymbol{X}_j)$ is the shape factor of each super particle.

3. Simulation results

Results of particle-MHD hybrid simulations of the kink instability and the fishbone instability are reported in this section. In the simulation, parameters are similar to the PDX experiments. The major radius is $R_0 = 1.43$ m and the minor radius is $a = 0.43$ m. The magnetic field at the axis is 1.5 T. The plasma density is taken to be uniform 5×10^{19} m^{-3}. The bulk plasma is hydrogen and the energetic ion is deuterium. The initial distribution of energetic ions in the velocity space is a slowing down distribution with the maximum energy 50 keV. The slowing down distribution is taken to be isotropic in the velocity space for simplicity. The spatial profile of energetic ion pressure is a Gaussian with pressure gradient scale length 0.15 m at the $q = 1$ surface, where q is the safety factor. Two runs where the central energetic ion beta values $\beta_h(0)$ are, 0 % and 3 %, respectively, were carried out.

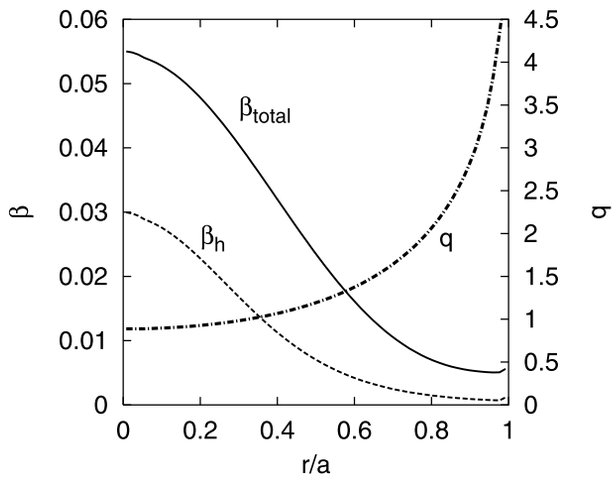

Fig. 1 Initial beta profiles and q-profile.

Figure 1 shows the initial beta profiles and q-profile for $\beta_h(0) = 3\%$. Figure 2 shows spatial profiles of the radial velocity v_r in the linear growth phase. Solid and dashed curves represent the sine and cosine part of the $m/n = 1/1$ harmonic, respectively. Here m is the poloidal mode number and n is the toroidal mode number. Dashed-dotted curves show the q-profile. In Fig. 2 the phase is chosen so as to maximize the sine part amplitude. The well-known top-hat structure of the kink mode is seen in Fig. 2(a). This mode is a purely MHD mode. For the central energetic ion beta value of 3 % a fishbone mode is destabilized. We have investigated energy evolution. Only the energetic ion energy is decreasing while the magnetic energy, MHD fluid kinetic energy, and MHD thermal energy are increasing. This clearly indicates that the instability is driven by the energetic ions. We can conclude that the instability is the fishbone instability. It can be seen in Fig. 2(b) that the spatial profile of the fishbone mode is different from that of the kink mode shown in Fig. 2(a).

For the fishbone instability, amplitude evolution of $m/n = 1/1$ harmonics of the radial velocity v_r is shown in Fig. 3(a). The frequency evolution of $m/n = 1/1$ harmonics of the radial magnetic field fluctuation is shown in Fig. 3(b). Frequency in the linear growth phase is 18 kHz which corresponds to $\omega \sim 3.5\times10^{-2} v_A/R_0$ and is close to the fishbone frequency in the PDX experiments, where ω is the fishbone mode frequency, and $\boldsymbol{v}_A$ is the Alfven velocity.

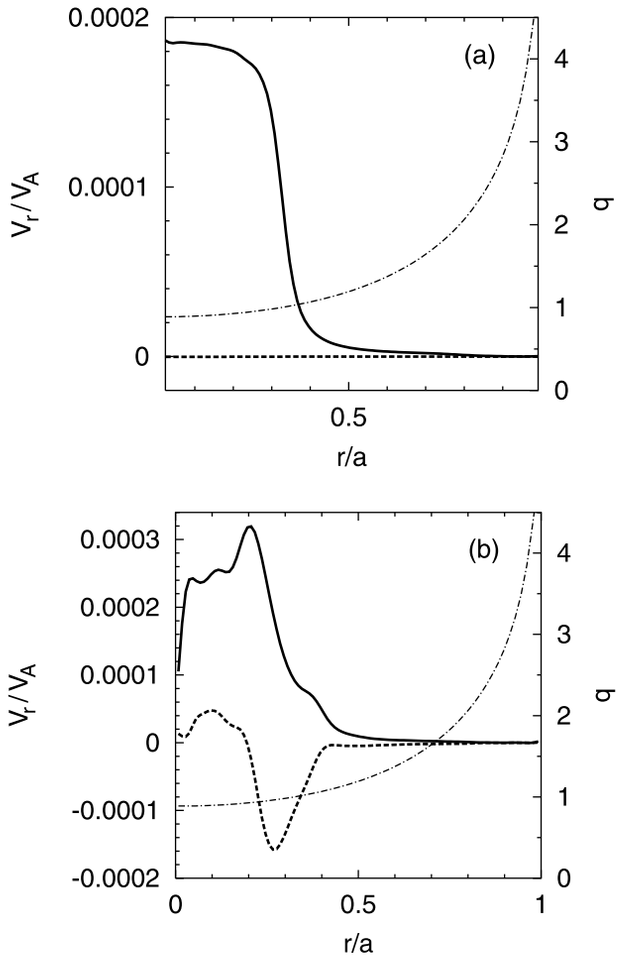

Fig. 2 Comparison in radial velocity spatial profiles of (a) kink mode for $\beta_h(0) = 0\,\%$ and (b) fishbone mode for $\beta_h(0) = 3\,\%$.
Solid and dashed curves represent the sine and cosine part of the $m/n = 1/1$ harmonic, respectively. Dashed-dotted curves show the q-profile.

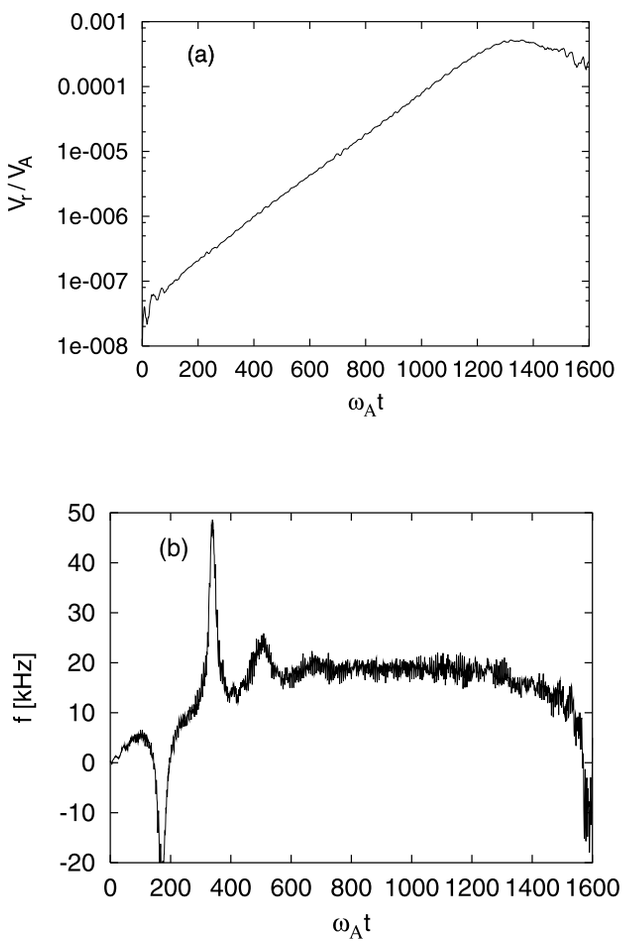

Fig. 3 (a) Amplitude evolution of $m/n = 1/1$ harmonic of the radial velocity v_r and (b) frequency evolution of $m/n = 1/1$ harmonic of the radial magnetic fluctuation δB_r.

The frequency shifts downward at saturation. The saturation level of the total velocity is $v/v_A \sim 2\times10^{-3}$. This gives the plasma displacement at the saturation $\xi \sim v/\omega \sim 5.7\times10^{-2}R_0 \sim 0.18a \sim 0.6r_{q=1}$, where $r_{q=1}$ denotes the minor radius of the magnetic surface where the safety factor is $q = 1$. Thus, the saturation level of the plasma displacement is comparable to the radius of the $q = 1$ surface. This saturation level is a factor of 7 larger than that found in the simulation of the thermal ion diamagnetic drift fishbone [4].

4. Discussion and summary

It was theoretically predicted in Ref. [7] that the fishbone mode has a two step structure and the width of the individual steps is a factor γ/ω smaller than the distance between them, where γ and ω are the growth rate and the real frequency of the mode, respectively. In the fishbone simulation results they are $\gamma \sim 8\times10^{-3}\omega_A$ and $\omega \sim 4\times10^{-2}\omega_A$, where $\omega_A = v_A/R_0$. The ratio is $\gamma/\omega \sim 0.2$. We can see a two step structure in Fig. 2(b), but it is not so clear as Ref. [7] predicts. We should notice that Ref. [7] assumed that no energetic particles are present around the $q = 1$ surface. In the simulation presented in this paper, energetic ions were distributed in a Gaussian form with regard to the minor radius and were present around the $q = 1$ surface. The energetic particles around the $q = 1$ surface in the present simulation might modify the two step structure. Another simulation where the energetic particles are absent from the $q = 1$ surface will be useful to test the conjecture.

In this paper we have investigated the preccessional fishbone instability using parameters similar to the PDX experiment. The spatial profile of the fishbone mode is different from the top-hat structure of the kink mode. The saturation of the fishbone instability and the frequency downshift have been demonstrated. The saturation level of the plasma displacement was comparable to the radius of the $q = 1$ surface. More work is needed to clarify the mechanism of saturation and frequency downshift.

References

[1] K. Mcguire, R. Goldston, M. Bell *et al*., Phys. Rev. Lett. **50**, 891 (1983).

[2] L. Chen, R.B. White and M.N. Rosenbluth, Phys. Rev. Lett. **52**, 1122 (1984).

[3] B. Coppi and F. Porcelli, Phys. Rev. Lett. **57**, 2272 (1986).

[4] J. Candy, H.L. Berk, B.N. Breizman and F. Porcelli, Phys. Plasmas **6**, 1822 (1999).

[5] Y. Todo and T. Sato, Phys. Plasmas **5**, 1321 (1998).

[6] S.E. Parker and W.W. Lee, Phys. Fluids B **5**, 77 (1993).

[7] A. Ödblom, B.N. Breizman, S.E. Sharapov, T.C. Hender and V.P. Pastukhov, Phys. Plasmas **9**, 155 (2002).